


**Dynamic Kosterlitz-Thouless theory for two-dimensional ultracold atomic gases**Zhigang Wu <sup>1,2</sup>, Shizhong Zhang,<sup>3</sup> and Hui Zhai<sup>4,5</sup><sup>1</sup>*Shenzhen Institute for Quantum Science and Engineering, Southern University of Science and Technology, Shenzhen 518055, Guangdong, China*<sup>2</sup>*Guangdong Provincial Key Laboratory of Quantum Science and Engineering, Southern University of Science and Technology, Shenzhen 518055, Guangdong, China*<sup>3</sup>*Department of Physics and HKU-UCAS Joint Institute for Theoretical and Computational Physics at Hong Kong, University of Hong Kong, Hong Kong, China*<sup>4</sup>*Institute for Advanced Study, Tsinghua University, Beijing, 100084, China*<sup>5</sup>*Center for Quantum Computing, Peng Cheng Laboratory, Shenzhen 518055, China*

(Received 30 June 2020; accepted 16 September 2020; published 7 October 2020)

In this paper we develop a theory for the first and second sounds in a two-dimensional atomic gas across the superfluid transition based on the dynamic Kosterlitz-Thouless theory. We employ a set of modified two-fluid hydrodynamic equations which incorporate the dynamics of the quantized vortices, rather than the conventional ones for a three-dimensional superfluid. As far as the sound dispersion equation is concerned, the modification is essentially equivalent to replacing the static superfluid density with a frequency-dependent one, renormalized by the frequency-dependent “dielectric constant” of the vortices. This theory has two direct consequences. First, because the renormalized superfluid density at finite frequencies does not display discontinuity across the superfluid transition, in contrast to the static superfluid density, the sound velocities vary smoothly across the transition. Second, the theory includes dissipation due to free vortices and thus naturally describes the sound-to-diffusion crossover for the second sound in the normal phase. With only one fitting parameter, our theory gives a perfect agreement with the experimental measurements of sound velocities across the transition, as well as the quality factor in the vicinity of the transition. The predictions from this theory can be further verified by future experiments.

DOI: [10.1103/PhysRevA.102.043311](https://doi.org/10.1103/PhysRevA.102.043311)**I. INTRODUCTION**

Topological defects, such as quantized vortices in superfluids, are of fundamental importance in physics of many two-dimensional (2D) systems [1]. Phase transitions driven by these defects, known as the Berezinskii-Kosterlitz-Thouless (BKT) transitions [2–6], are found to exist in a wide range of 2D systems [6], including helium films [7,8], superconducting films [9], and 2D ultracold atomic gases [10,11]. Although conceptually similar to the other two kinds of systems, the study of ultracold atomic gases can in fact significantly enrich the BKT physics [12]. From the perspective of experimental technique, for example, matter wave interferometry allows visualization of quantized vortices and thus potentially direct observation of the proliferation of free vortices across the BKT transition [12].

Nevertheless, a more important conceptual aspect is the study of sound propagation, which behaves very differently in these systems. In the superconducting films, the sound wave corresponds to a plasma mode with the square-root dispersion due to the Coulomb interaction between charged electrons [13,14]. As for the helium films, because they form on a substrate which clamps the motion of the normal component, and because they are almost incompressible, the only type of sound allowed is a surface wave of the superfluid component

known as the third sound [15–17]. The 2D atomic gas, on the other hand, is charge neutral compared to superconducting films; it is also isolated from any other environment and is much more compressible compared to helium films, which permits motions of both the normal and superfluid components. Thus, the cold atomic gas provides a platform for the experimental exploration of both the first and second sounds in a 2D system across the BKT transition.

Indeed, such an experiment has been carried out recently in a ultracold 2D Bose gas [18]. However, a discrepancy is found between the experimental observation and the theories based on the Landau two-fluid theory [18–21]. Since the static superfluid density has a discontinuous jump across the BKT transition, the standard Landau two-fluid theory naturally predicts a discontinuity of the second sound velocity across the BKT transition. However, such a discontinuity is not found in the experiment. Instead, the experiment finds a second sound mode with a smoothly varying velocity and a rapidly increasing damping rate across the BKT transition. Although several theoretical works offer possible explanations with various numerical approaches [22–24], most of them assume that the experimental system is in the collisionless regime rather than the hydrodynamic regime. Thus it remains an open question as to whether the sound propagation in the actual physical system, whose collision rate is several times larger than the

probed sound frequencies [18], can still be understood in term of hydrodynamics.

This discrepancy thus calls for a serious revisit of the two-fluid hydrodynamics for 2D BKT superfluids. In fact, earlier pioneering works have developed a so-called dynamic Kosterlitz-Thouless (KT) theory [25–28] to understand the dynamics and the third sound propagation in helium films, which shows that a proper treatment of the vortex dynamics is crucial, especially in the vicinity of the superfluid transition. However, such a contribution from vortex dynamics is not contained in the standard Landau two-fluid hydrodynamic theory [29]. Because the contribution of vortex dynamics is much more significant in two dimensions than in three, this explains why the Landau two-fluid theory works well in three dimensions [30–36] but fails in two. So far, a dynamic KT theory for the first and second sound propagation in 2D atomic gases is still lacking.

In this paper we present such a theory, and we show that the experimental findings can be well explained within the framework of hydrodynamic theory when the vortex dynamics is properly taken into account. The key result of our theory is a dispersion equation that determines the velocity and damping of both branches of the sound. Based on this equation, we show that both sound velocities vary smoothly across the BKT transition at finite probing frequencies. For the second sound in particular, we also show that the damping increases rapidly above the BKT transition due to the proliferation of free vortices, eventually turning the wave propagation into a diffusive mode. With only one fitting parameter, our theory agrees quantitatively with experimental measurements of a set of second sound velocities across the BKT transition, as well as the quality factor in the vicinity of the transition.

The rest of the paper is organized as follows. In Sec. II we develop the hydrodynamic theory for 2D atomic superfluids which incorporates the dynamics of the vortices described by the dynamic KT theory. A sound dispersion equation is derived and compared to that for the three-dimensional (3D) superfluid. In Sec. III we analyze this sound dispersion equation and discuss two general features of the sound modes at finite frequencies, i.e., continuity of sound velocities across the BKT transition and second sound to diffusion crossover. The full solution of this equation is presented in Sec. IV, where comparisons to experimental results and further predictions of the theory are given. All the main results are summarized in Sec. V.

## II. HYDRODYNAMIC THEORY AND SOUND DISPERSION EQUATION

We begin by deriving a sound dispersion equation for 2D atomic superfluids from a set of five basic hydrodynamic equations. The first three of them are essentially the conservation laws of mass, momentum, and entropy,

$$\frac{\partial \rho}{\partial t} = -\nabla \cdot \mathbf{j}, \quad (1)$$

$$\frac{\partial \mathbf{j}}{\partial t} = -\nabla P, \quad (2)$$

$$\frac{\partial(\rho s)}{\partial t} = -\nabla \cdot (\rho s \mathbf{v}_n), \quad (3)$$

where  $\rho$  is the mass density,  $\mathbf{j}$  is the mass current,  $P$  is the pressure, and  $s$  is the entropy per unit mass. In terms of the “bare” superfluid density  $\rho_s^0$  and the “bare” normal fluid density  $\rho_n^0$ , we can write

$$\rho = \rho_s^0 + \rho_n^0, \quad \mathbf{j} = \rho_s^0 \mathbf{v}_s + \rho_n^0 \mathbf{v}_n,$$

where  $\mathbf{v}_s$  and  $\mathbf{v}_n$  are the superfluid and normal fluid velocity fields, respectively. These “bare” densities contain only effects of short wavelength fluctuations, in contrast to the renormalized ones introduced later in Eqs. (8) and (9). The three equations above are the same as those in the Landau two-fluid hydrodynamics.

The fourth equation is the equation of motion for the superfluid component [25]

$$\frac{\partial \mathbf{v}_s}{\partial t} + \hat{z} \times \mathbf{J}_v = -\nabla \mu, \quad (4)$$

where  $\mu$  is the local chemical potential and  $\mathbf{J}_v$  is the current of the quantized vortices to be defined shortly. The second term in Eq. (4), absent in the corresponding equation for the 3D superfluids, accounts for the contribution of the quantized vortices in 2D superfluids. The density of quantized vortices can be written as  $N(\mathbf{r}, t) = (2\pi \hbar/m) \sum_i n_i \delta[\mathbf{r} - \mathbf{r}_i(t)]$ , where  $\mathbf{r}_i$  is the position of the  $i$ th vortex and  $n_i = \pm 1$  describes the direction of circulation for this vortex. Then  $\mathbf{J}_v(\mathbf{r}, t)$  can be defined as  $\mathbf{J}_v(\mathbf{r}, t) = (2\pi \hbar/m) \sum_i n_i (d\mathbf{r}_i/dt) \delta[\mathbf{r} - \mathbf{r}_i(t)]$ , such that the vortices obey the equation of continuity  $\partial N(\mathbf{r}, t)/\partial t = -\nabla \cdot \mathbf{J}_v$ . By viewing vortices as charged particles and drawing on an analogy to a 2D plasma, it can be shown that  $\mathbf{J}_v(\mathbf{r}, t)$  is related to the relative velocity fields of the superfluid and normal fluid component via an “Ohm’s law” [25,27]

$$\mathbf{J}_v(\mathbf{r}, t) = \int dt' \sigma(t-t') \hat{z} \times [\mathbf{v}_n(\mathbf{r}, t') - \mathbf{v}_s(\mathbf{r}, t')], \quad (5)$$

where  $\sigma$  is a complex “conductivity” for the vortices under the “electric field”  $\hat{z} \times (\mathbf{v}_n - \mathbf{v}_s)$ . In the frequency space,  $\sigma$  can be written in terms of the dynamic “dielectric constant”  $\epsilon(\omega)$  as

$$\sigma(\omega) = -i\omega[\epsilon(\omega) - 1]. \quad (6)$$

Equations (1)–(5) form a complete set of basic hydrodynamic equations for the 2D superfluid. Considering small deviations of relevant physical quantities from their equilibrium values and following standard derivations, we arrive at the following sound dispersion equation (see Appendix A):

$$\left[ \frac{\omega^2}{k^2} - \frac{1}{\rho \kappa_T} \right] \left[ \frac{\omega^2}{k^2} - \frac{T s^2 \rho_s(\omega)}{c_v \rho_n(\omega)} \right] - \frac{1}{\rho} \left( \frac{1}{\kappa_s} - \frac{1}{\kappa_T} \right) \frac{\omega^2}{k^2} = 0, \quad (7)$$

where  $\kappa_T = \rho^{-1}(\partial \rho / \partial P)_T$  and  $\kappa_s = \rho^{-1}(\partial \rho / \partial P)_s$  are the isothermal and isoentropic compressibility, respectively, and  $c_v = T(\partial s / \partial T)_\rho$  is the specific heat at constant volume. Here we introduce the frequency-dependent superfluid and normal density as

$$\rho_s(\omega) = \frac{\rho_s^0}{\epsilon(\omega)}, \quad (8)$$

$$\rho_n(\omega) = \rho - \rho_s(\omega). \quad (9)$$

Note that the physical densities  $\rho$ ,  $\rho_s^0$  and the entropy  $s$  entering Eqs. (7)–(9) all take their equilibrium values.

Equation (7), which determines the dispersions of the sound propagation in the 2D superfluid, represents the central result of this paper. Remarkably, despite the modification of one hydrodynamic equation and the addition of another, the resulting sound dispersion equation (7) has nearly an identical form as its 3D superfluid counterpart [29], the only difference being that the static superfluid and normal density are now replaced by the frequency-dependent densities defined in Eqs. (8) and (9). In other words, by explicitly including the vortex dynamics in the hydrodynamic equations, the effect on sound dispersion is equivalent to renormalizing the bare superfluid density by the frequency-dependent dielectric constant of quantized vortices. In fact, by setting the dynamic dielectric constant  $\epsilon(\omega) = 1$  in the absence of vortices, Eq. (7) immediately reduces to the familiar sound dispersion equation in the 3D Landau two-fluid theory. For 2D superfluid,  $\epsilon(\omega)$  is generally complex, meaning that the presence of the quantized vortices in such systems not only modifies the sound velocity but also induces the damping.

### III. GENERAL FEATURES OF THE SOUND MODES AT FINITE WAVE VECTORS

Before proceeding to more detailed calculations, we first discuss two general features of the sound modes predicted by the dynamic KT theory, which can be inferred from the general properties of  $\epsilon(\omega)$  (see Appendix B) and Eq. (7). For this purpose, we express the solutions to Eq. (7) as

$$\omega_\alpha(k) = \varpi_\alpha(k) + i\gamma_\alpha(k), \quad (10)$$

where  $\varpi_\alpha(k)$  and  $\gamma_\alpha(k)$  are the real and imaginary parts of the dispersion, respectively, and  $\alpha = 1, 2$  denotes the two sound branches. As in the experiment [18], the velocity of sound here is defined as

$$c_\alpha = \varpi_\alpha(k)/k \quad (11)$$

at some experimental wave vector  $k$ .

#### A. Continuity of sound velocities

The determination of the dynamic dielectric constant  $\epsilon(\omega)$  due to the vortices is crucial to solving Eq. (7) for the first and second sound dispersion. According to the KT theory, bound vortex pairs of all separations populate in the superfluid below the critical temperature  $T_c$ . These vortex pairs are similar to the electric dipoles in the 2D plasma in the sense that they can be polarized by the flow of the fluid, resulting in a counterflow which effectively reduces (or renormalizes) the bare superfluid density. The renormalized static superfluid density is given by

$$\rho_s = \rho_s^0 / \tilde{\epsilon}(r = \infty, T), \quad (12)$$

where  $\tilde{\epsilon}(r, T)$  is the static, length, and temperature-dependent dielectric constant describing the polarizability of vortex pairs separated by distance  $r$ . As the temperature increases and surpasses  $T_c$ , the vortex pairs with largest separations begin to suddenly dissociate into free vortices; i.e.,  $\tilde{\epsilon}(r = \infty, T_c^-)$  is finite while  $\tilde{\epsilon}(r = \infty, T_c^+)$  diverges. This leads to a precipitous drop of the static superfluid density from a finite value to zero at  $T_c$  and a breakdown of dissipationless flow for  $T > T_c$ .

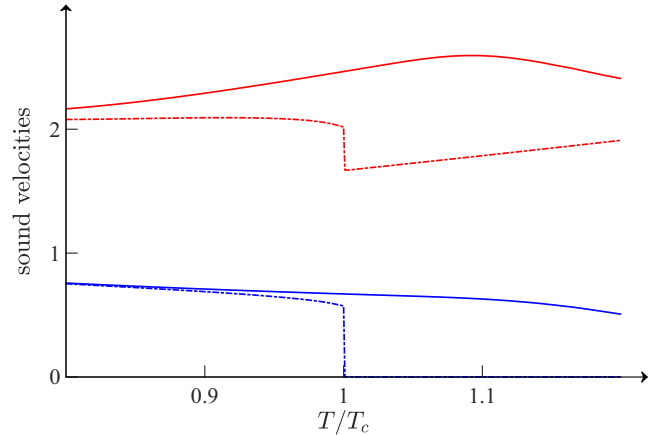


FIG. 1. Velocity of the first (upper curves) and second sound (lower curves) as a function of temperature for a 2D superfluid of weakly interacting bosons across the BKT transition: our dynamic KT theory (solid lines) vs the Landau two-fluid theory (dashed lines). The results of the dynamic KT theory are calculated for a specific experimental wave vector  $k_0$  and using actual parameters of a weakly interacting Bose gas [18]. The sound velocities shown are in units of the Bogoliubov sound velocity.

The above physical picture was later generalized to account for dynamic situations in the so-called dynamic KT theory [25–27], where  $\epsilon(\omega)$  was introduced to characterize the response of bound vortex pairs and free vortices to oscillating velocity fields at frequency  $\omega$  in the long wavelength limit. It can be shown that [27] (see also Appendix B)

$$\lim_{\omega \rightarrow 0} \epsilon(\omega, T) = \tilde{\epsilon}(r = \infty, T). \quad (13)$$

Thus the static superfluid density in Eq. (12) is nothing but the zero-frequency component of the frequency-dependent superfluid density in Eq. (8).

Here we should emphasize the critical difference between  $\epsilon(\omega)$  at zero frequency  $\epsilon(\omega = 0)$  and  $\epsilon(\omega)$  at finite frequencies. At  $\omega = 0$ ,  $\epsilon(\omega = 0)$  is real and finite for  $T < T_c$  but immediately diverges at  $T = T_c^+$ , where  $T_c$  is the BKT transition temperature. Hence, the nonanalyticity of  $\epsilon(\omega = 0)$  as a function of the temperature leads to a finite  $\rho_s(\omega = 0)$  at  $T_c^-$  but a vanishing  $\rho_s(\omega = 0)$  at  $T_c^+$ . Since the conventional Landau two-fluid theory uses the static superfluid density  $\rho_s(\omega = 0)$  in the hydrodynamic equations, it predicts a discontinuity in sound velocities as a result of the sudden jump of  $\rho_s(\omega = 0)$  at  $T_c$  [19,21]. If  $\kappa_s = \kappa_T$ , the density and temperature fluctuations are decoupled and the discontinuity exists only in the second sound, i.e., the temperature wave. Generally,  $\kappa_s \neq \kappa_T$ , so the aforementioned two types of fluctuations are coupled and the discontinuity exists in both sound modes, as shown in Fig. 1 by the dashed lines. For any finite  $\omega$ , however,  $\epsilon(\omega)$  is always finite and is a smooth function of  $T$  across BKT transition. This leads to smooth sound velocities in the first and the second sounds. As an illustration, we calculate the sound velocities probed at finite frequencies from Eq. (7) using actual parameters of a weakly interacting 2D Bose gas, and the results are shown by solid lines in Fig. 1.

### B. Second sound to diffusion crossover

The second general feature our theory predicts is the second sound to diffusion crossover as a result of the proliferation of free vortices above  $T_c$ . In the temperature regime slightly above  $T_c$ , the dielectric constant can be written as [25] (see also Appendix B)

$$\epsilon(\omega) \approx \epsilon_b + i\sigma_f/\omega, \quad (14)$$

where  $\epsilon_b$  is the bound vortex pair contribution to the dielectric constant and  $\sigma_f$  accounts for the ‘‘conductivity’’ of free vortices. Now  $\epsilon_b$  itself is complex and a function of both  $\omega$  and  $T$ . However, for our qualitative discussions here, it can be treated as a real constant since it is slowly varying in the vicinity of  $T_c$  and  $\text{Im}\epsilon_b \ll \text{Re}\epsilon_b$ . More specifically, we will make the approximation  $\epsilon_b \approx \epsilon(\omega = 0, T_c^-)$  in demonstrating the second sound to diffusion crossover. The free vortex ‘‘conductivity’’  $\sigma_f(T)$  is real and proportional to the density of free vortices. Thus it vanishes in the superfluid regime and increases rapidly as the temperature increases above  $T_c$  due to the proliferation of free vortices.

For clarity, let us first demonstrate the crossover for a simple situation with  $\kappa_s = \kappa_T$  in Eq. (7), where the second sound corresponds to a pure temperature wave governed by the following equation:

$$\omega^2 - 2i\gamma_2\omega - u_2^2k^2 = 0, \quad (15)$$

where  $\gamma_2 \equiv -\frac{\rho\sigma_f}{2(\rho\epsilon_b - \rho_s^0)}$  and  $u_2 \equiv \sqrt{\frac{Ts^2\rho_s^0}{c_v(\rho\epsilon_b - \rho_s^0)}}$ . The solution of this equation can be easily obtained as

$$\omega_2(k) = \sqrt{u_2^2k^2 - \gamma_2^2} + i\gamma_2. \quad (16)$$

From Eq. (16) we can immediately define a threshold wave vector  $k^*(T) \equiv |\gamma_2/u_2|$  such that the second sound is a damped sound for  $k > k^*(T)$  and becomes purely diffusive for  $k < k^*(T)$ . In other words, we can define a  $k$ -dependent temperature  $T^*(k)$  whereby the second sound with wave vector  $k$  becomes purely diffusive for  $T > T^*(k)$ . Since the damping parameter  $\gamma_2$ , proportional to  $\sigma_f(T)$ , vanishes below  $T_c$ ,  $T^*(k)$  must be greater than  $T_c$  for any finite  $k$ . That is to say, the sound-to-diffusion crossover occurs in the normal phase. In the general case of  $\kappa_s \neq \kappa_T$ , we again use Eq. (14) in the sound dispersion equation (7) and arrive at the following quartic equation:

$$\omega^4 - 2i\gamma_2\omega^3 - (u_1^2 + u_2^2 + \delta\kappa)k^2\omega^2 + 2i\gamma_2(u_1^2 + \delta\kappa)k^2\omega + u_1^2u_2^2k^4 = 0, \quad (17)$$

where  $u_1 \equiv \sqrt{1/\rho\kappa_T}$  and  $\delta\kappa \equiv (\kappa_T - \kappa_s)/\rho\kappa_s\kappa_T$ . The above quartic equation can be easily solved numerically to obtain  $\omega_\alpha(k)$  for any specific  $T$ . For sufficiently large  $k$ , we find that the four complex solutions can be organized into two pairs, each of which has two solutions with opposite real parts. We can thus identify the two solutions with positive real parts, one in each pair, as the dispersions for the two branches of the sound. As we decrease  $k$ , the real part of the solution corresponding to the second sound decreases gradually and becomes zero for  $k < k^*(T)$ . In other words, we find purely imaginary solutions for the second sound branch for  $k < k^*(T)$ , signaling that the sound mode transitions into a

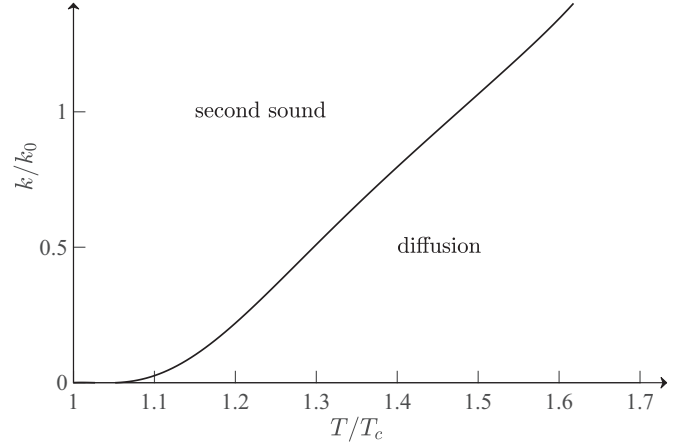


FIG. 2. A sound-to-diffusion crossover in the  $k$ - $T$  plane for the second sound, predicted by our dynamic KT theory for a 2D superfluid of weakly interacting bosons above the BKT transition. Again, the boundary separating the second sound and diffusion regime is calculated using actual parameters of a weakly interacting Bose gas [18], where  $k_0$  is the wave vector at which the experimentally probed sound propagates.

diffusive mode, which is similar to the more special case of  $\kappa_s = \kappa_T$ . In Fig. 2 we show an example of the second sound to diffusion boundary in the  $k$ - $T$  plane defined by  $\varpi_2(k) = 0$ , again using the actual parameters for a 2D weakly interacting Bose gas.

### IV. EXPERIMENTAL COMPARISONS AND PREDICTIONS

In this section we turn to full numerical solutions to Eq. (7) and compare the results with the experiment. The solutions to Eq. (7) can be formally written in the following form:

$$\varpi_\alpha + i\gamma_\alpha = v_\alpha(\varpi_\alpha + i\gamma_\alpha). \quad (18)$$

Here

$$v_\alpha(\omega) = \frac{1}{\sqrt{2}} \left\{ u_1^2 + u_2^2(\omega) + \delta\kappa - (-1)^\alpha \sqrt{[u_1^2 + u_2^2(\omega) + \delta\kappa]^2 - 4u_1^2u_2^2(\omega)} \right\}^{1/2}, \quad (19)$$

where  $u_1 \equiv \sqrt{\frac{1}{\rho\kappa_T}}$ ,  $u_2(\omega) \equiv \sqrt{\frac{1}{\rho\kappa_T} \frac{Ts^2}{c_v} [\rho_s(\omega)/\rho_n(\omega)]}$  and  $\delta\kappa \equiv (\kappa_T - \kappa_s)/\rho\kappa_s\kappa_T$ . The  $u_2(\omega)$  function defined here is the frequency-dependent generalization of the  $u_2$  parameter introduced earlier in Eq. (15). Note that  $u_2(\omega)$  is complex even for real arguments because  $\rho_s(\omega)$  and  $\rho_n(\omega)$  are complex. To solve for the dispersion, we need to (1) determine thermodynamic quantities, i.e.,  $s$ ,  $\kappa_s$ ,  $\kappa_T$ ,  $c_v$ , in term of microscopic parameters, (2) calculate the dynamic dielectric function  $\epsilon(\omega)$  and from that  $\rho_s(\omega)$  and  $\rho_n(\omega)$  for any complex  $\omega$ , and (3) iterate Eq. (18) self-consistently to obtain the real and imaginary parts of the spectrum  $\varpi_\alpha(k)$  and  $\gamma_\alpha(k)$ .

For 2D ultracold Bose gases, the thermodynamic quantities can be calculated in terms of certain universal functions which depend solely on the dimensionless interaction constant  $g$  and the ratio of chemical potential to temperature  $\mu/T$  [37,38]. In addition, the dielectric constant  $\epsilon(\omega)$  can be evaluated via

TABLE I. Various physical quantities (the first column) needed for solving the sound dispersion equation. The second column lists the microscopic parameters that these physical quantities depend on. The third column lists the corresponding equations for calculating these quantities given in the Appendixes.

Quantities	Parameters	Appendix
$\rho_s^0$	$g, \mu/T$	(B1)–(B4)
$\epsilon(\omega)$	$g, \mu/T, l_D, \omega$	(B5)–(B8)
$s, \kappa_s, \kappa_T, c_v$	$g, \mu/T$	(C1)–(C2)

the dynamic KT theory. Although the calculations of all these quantities are rather involved, they are well documented in the literature [19,25,27,39] and the details will be relegated to the Appendixes. Here we shall tabulate only all the parameters needed for solving the sound dispersion equation in Table I, and we refer readers interested in details of the calculation to the corresponding equations in the Appendixes.

The main microscopic parameter in determining  $\epsilon(\omega)$  is a dimensionless quantity,

$$l_D \equiv \ln \sqrt{2D/\omega_0 a_0^2}, \quad (20)$$

where  $D$  is the vortex diffusion constant,  $a_0$  is the vortex core size, and  $\omega_0 = c_B k_0$  is the typical frequency associated with sound propagation. Here  $c_B = \sqrt{g\rho}/m^{3/2}$  is the Bogoliubov sound velocity and  $k_0 = \pi/L$  is the wave vector of the probed sound for a system of size  $L$ . Since there is no reliable method to calculate the diffusion constant  $D$ , we shall use  $l_D$  as the only fitting parameter when comparing our theoretical results to the experimental measurements. We adjust  $l_D$  so as to minimize

$$\delta = \sum_i |c_2(T_i) - c_{\text{exp}}(T_i)|^2, \quad (21)$$

where  $c_2(T_i)$  and  $c_{\text{exp}}(T_i)$  are the theoretical and experimental values of the second sound velocity at temperature  $T_i$ , respectively. The resulting second sound velocity is shown in Fig. 3, where very good agreements between theory and experiment are obtained. Using  $l_D$  obtained in this fitting, we find the quality factor of the second sound  $Q \equiv |\varpi_2/\gamma_2| \sim 9$  at  $T_c$ , consistent with the experimental value of  $\sim 8$ . This further justifies that the value of  $l_D$  found from the fitting is a reasonable one. However, our theoretical values of  $Q$  become significantly larger than the experimental measurements for temperatures deep in the superfluid phase. This is because the damping due to free vortices is the only damping mechanism included in this hydrodynamics theory. Deep in the superfluid phase, where the vortex contribution is insignificant, our theory recovers the dissipationless hydrodynamics and as a result underestimates the damping.

Although the sound velocity is calculated at the experimental wave vector  $k_0$ , i.e.,  $c_2 = \varpi_2(k_0)/k_0$ , we have checked that its value does not depend on  $k$  for  $k > k_0$ . In other words, the linear dispersion of the sound is well established by our theory. The second sound damping, however, has a strong dependence on the wave vector. At  $T_c$ , the second sound damping is found to increase approximately as  $\sim k^2$  for  $k > k_0$ . Thus the quality factor  $Q$  increases linearly in  $k$ , as

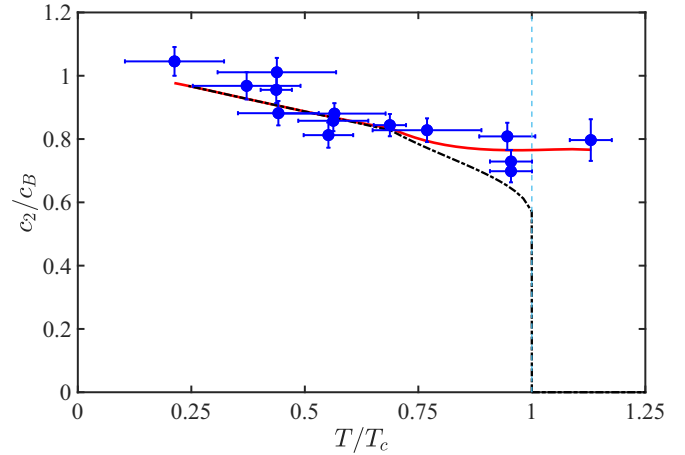


FIG. 3. Second sound velocity  $c_2/c_B$  as a function of temperature  $T/T_c$  calculated for a weakly interacting 2D  $^{87}\text{Rb}$  gas with  $g = 0.16$ . The symbols are the experimental results [18]. The solid line is our theory with  $l_D = -1.14$ , and the dashed line is the Landau two-fluid theory. Here  $c_B = \sqrt{g\rho}/m^{3/2}$  is the Bogoliubov sound velocity.

shown in Fig. 4. This is another important prediction from our theory, which, together with the sound to diffusion transition, can be tested in future experiments.

## V. CONCLUDING REMARKS

In summary, we have developed a dynamic KT theory to understand the finite frequency sound propagation in 2D ultracold Bose gases in the hydrodynamic regime. Building on the conventional two-fluid hydrodynamic framework, this theory takes into account the finite frequency responses of the vortices to oscillating velocity fields, described by the complex dynamic dielectric constant. Such dynamic responses essentially renormalize the superfluid density by the dynamic dielectric constant, which removes the discontinuity in the superfluid density and introduces dissipation due to bound and free vortices. This in turn leads to smooth-varying sound velocities across the BTK transition and sound-to-diffusion

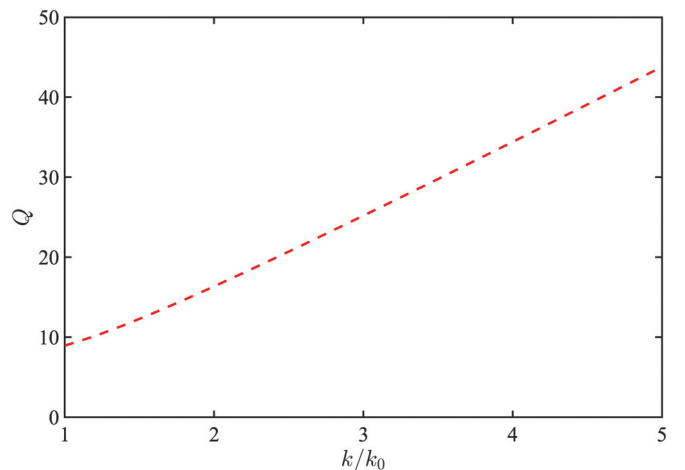


FIG. 4. The second sound quality factor  $Q(k)$  as a function of the wave vector  $k$  at  $T_c$ . The parameters are the same as in Fig. 3.

crossover for the second sound in the normal phase. With one fitting parameter, our calculations of the second sound velocity and damping are in good agreement with a recent experiment on the weakly interacting 2D Bose gas. Furthermore, by varying the probing wave vector, our prediction of the second sound to diffusion crossover and of the wave vector dependence of the quality factor can be straightforwardly tested in future experiments. Finally, our theory can be extended to the study of 2D Fermi superfluids with a BEC-BCS crossover.

### ACKNOWLEDGMENTS

We acknowledge helpful discussions with Zhiyuan Yao, Pengfei Zhang, and Mingyuan Sun. Z.W. is supported by the NSFC (Grant No. 11974161), Key Area Research and Development Program of Guangdong Province (Grant No. 2019B030330001), and Guangdong Provincial Key Laboratory (Grant No. 2019B121203002). S.Z. is supported by HK GRF 17318316 and 17305218 and CRF C6026-16W and C6005-17G, and the Croucher Foundation under the Croucher Innovation Award. H.Z. acknowledges support by the Beijing Distinguished Young Scientist Program, MOST (Grant No. 2016YFA0301600), and NSFC (Grant No. 11734010).

### APPENDIX A: DERIVATION OF THE SOUND DISPERSION EQUATION

The first hydrodynamic sound equation can be obtained from combining Eqs. (1) and (2). Considering small deviations of the relevant physical quantities from their equilibrium values, we find from Eqs. (1) and (2)

$$\frac{\partial^2 \delta \rho}{\partial t^2} - \nabla^2 \delta P = 0, \quad (\text{A1})$$

where  $\delta \rho$  and  $\delta P$  are variations of the total density and the pressure, respectively. The variation of the pressure can be expressed in terms of those of the density and the temperature as follows:

$$\begin{aligned} \delta P &= \left( \frac{\partial P}{\partial \rho} \right)_T \delta \rho + \left( \frac{\partial P}{\partial T} \right)_\rho \delta T \\ &= \frac{1}{\rho \kappa_T} \delta \rho + \frac{\alpha_P}{\kappa_T} \delta T, \end{aligned} \quad (\text{A2})$$

where  $\kappa_T = \frac{1}{\rho} \left( \frac{\partial \rho}{\partial P} \right)_T$  is the isothermal compressibility and  $\alpha_P = -\frac{1}{\rho} \left( \frac{\partial \rho}{\partial T} \right)_P$  is the isobaric thermal expansion coefficient. Substitution of the above equation into Eq. (A1) yields

$$\frac{\partial^2 \delta \rho}{\partial t^2} - \frac{1}{\rho \kappa_T} \nabla^2 \delta \rho - \frac{\alpha_P}{\kappa_T} \nabla^2 \delta T = 0. \quad (\text{A3})$$

In terms of the Fourier components of the density and temperature fluctuations, we find the first hydrodynamic sound equation:

$$\left( \frac{\omega^2}{k^2} - \frac{1}{\rho \kappa_T} \right) \delta \rho(\mathbf{k}, \omega) - \frac{\alpha_P}{\kappa_T} \delta T(\mathbf{k}, \omega) = 0. \quad (\text{A4})$$

To obtain the second hydrodynamic sound equation, we first linearize Eq. (3) and use Eq. (1) to obtain

$$\frac{\partial \delta s}{\partial t} = -s \frac{\rho_s^0}{\rho} \nabla \cdot (\mathbf{v}_n - \mathbf{v}_s). \quad (\text{A5})$$

Using the thermodynamic relation

$$\begin{aligned} \delta s &= \left( \frac{\partial s}{\partial T} \right)_\rho \delta T + \left( \frac{\partial s}{\partial \rho} \right)_T \delta \rho \\ &= \frac{c_v}{T} \delta T - \frac{\alpha_P}{\rho^2 \kappa_T} \delta \rho, \end{aligned} \quad (\text{A6})$$

where  $c_v = (\partial s / \partial T)_\rho / T$  is the specific heat at constant volume, Eq. (A5) can be written as

$$\frac{c_v}{T} \frac{\partial \delta T}{\partial t} - \frac{\alpha_P}{\rho^2 \kappa_T} \frac{\partial \delta \rho}{\partial t} = -s \frac{\rho_s^0}{\rho} \nabla \cdot \mathbf{v}_{ns}, \quad (\text{A7})$$

where we define the relative velocity field  $\mathbf{v}_{ns} = \mathbf{v}_n - \mathbf{v}_s$ . Fourier transforming the above equation gives

$$-i\omega \left[ \frac{c_v}{T} \delta T(\mathbf{k}, \omega) - \frac{\alpha_P}{\rho^2 \kappa_T} \delta \rho(\mathbf{k}, \omega) \right] = -is \frac{\rho_s^0}{\rho} \mathbf{k} \cdot \mathbf{v}_{ns}(\mathbf{k}, \omega). \quad (\text{A8})$$

Next, we use the Gibbs-Duhem equation

$$\delta \mu = \frac{1}{\rho} \delta P - s \delta T \quad (\text{A9})$$

and Eq. (2) to rewrite Eq. (4) as

$$\frac{\rho_n^0}{\rho} \frac{\partial}{\partial t} \hat{z} \times \mathbf{v}_{ns} + \mathbf{J}_v = -s \hat{z} \times \nabla \delta T. \quad (\text{A10})$$

In momentum frequency space we have

$$\frac{\rho_n^0}{\rho} (-i\omega) \hat{z} \times \mathbf{v}_{ns}(\mathbf{k}, \omega) + \mathbf{J}_v(\mathbf{k}, \omega) = -is \hat{z} \times \mathbf{k} \delta T(\mathbf{k}, \omega). \quad (\text{A11})$$

To close the above equation, we need Eq. (5), which, in Fourier space, is

$$\begin{aligned} \mathbf{J}_v(\mathbf{k}, \omega) &= \sigma(\omega) \hat{z} \times \mathbf{v}_{ns}(\mathbf{k}, \omega) \\ &= -i\omega [\epsilon(\omega) - 1] \hat{z} \times \mathbf{v}_{ns}(\mathbf{k}, \omega), \end{aligned} \quad (\text{A12})$$

where in the second line expressed the complex conductivity  $\sigma$  in terms of the dielectric constant. Substituting the above expression into Eq. (A11) and multiplying both sides by  $\mathbf{k}$  we arrive at

$$-i\omega \left[ \epsilon(\omega) - \frac{\rho_s^0}{\rho} \right] \mathbf{k} \cdot \mathbf{v}_{ns}(\mathbf{k}, \omega) = -isk^2 \delta T(\mathbf{k}, \omega). \quad (\text{A13})$$

Now we use Eq. (A13) to eliminate the  $\mathbf{k} \cdot \mathbf{v}_{ns}(\mathbf{k}, \omega)$  term in Eq. (A8), and we find the second hydrodynamic sound equation:

$$\begin{aligned} &\frac{\alpha_P}{\rho^2 \kappa_T} \frac{\omega^2}{k^2} \delta \rho(\mathbf{k}, \omega) \\ &= - \left[ \frac{\rho_s^0}{\rho} s^2 \frac{1}{\epsilon(\omega) - \rho_s^0 / \rho} - \frac{c_v}{T} \frac{\omega^2}{k^2} \right] \delta T(\mathbf{k}, \omega). \end{aligned} \quad (\text{A14})$$

Combining the two hydrodynamic sound equations (A4) and (A14), we finally arrive at Eq. (7), which determines the dispersion of sound propagation in 2D atomic superfluids.

### APPENDIX B: DYNAMIC DIELECTRIC CONSTANT

As we shall see, the necessary ingredients for calculating  $\epsilon(\omega)$  are  $\tilde{\epsilon}(r, T)$  and  $\xi(T)$ , the latter of which is a correlation length specifying the size of the largest vortex pairs. Both of

the quantities can be determined from the well-known KT recursion relations in terms of three microscopic parameters: the bare coupling constant  $K_0 = (\hbar/m)^2 \rho_s^0 / (k_B T)$ , the vortex core diameter  $a_0$ , and the bare vortex fugacity  $y_0 = \exp\{-\lambda K_0\}$  [4]. Averaging the system over vortex pairs with separation smaller than  $a_0 e^l$  gives rise to parameters  $K(l)$  and  $y(l)$  determined by the recursion relations

$$\begin{aligned} \frac{d}{dl} [K(l)]^{-1} &= 4\pi^3 y^2(l), \\ \frac{d}{dl} y(l) &= [2 - \pi K(l)] y(l), \end{aligned} \quad (\text{B1})$$

where  $K(l=0) = K_0$  and  $y(l=0) = y_0$ . The scale-dependent static dielectric constant  $\tilde{\epsilon}(r)$  is defined as

$$\tilde{\epsilon}(r) = K_0 / K[l = \ln(r/a_0)]. \quad (\text{B2})$$

To calculate  $\tilde{\epsilon}(r)$  we need to know  $\lambda$  and  $K_0$  (or equivalently  $\rho_s^0$ ). Currently, the best theoretical estimate for the former is  $\lambda = \pi^2/4$  [40]. As for  $K_0$  or  $\rho_s^0$ , we use the recursion relation to infer its value since we have

$$\begin{aligned} K(l = \infty) &= (\hbar/m)^2 \rho_s(0) / (k_B T) \\ &= \frac{1}{2\pi} \mathcal{D}_s. \end{aligned} \quad (\text{B3})$$

In other words, once we know  $\rho_s(\omega=0)$  from calculating  $\mathcal{D}_s$ , we can deduce  $\rho_s^0$  using the recursion relation. Next, the correlation length  $\xi(T)$  is defined as the size of the largest vortex pairs and is thus infinite below  $T_c$  and finite above. More specifically, above  $T_c$ ,  $\xi(T)$  is determined as the length scale at which  $y(l)$  becomes comparable to  $y_0$ , namely,

$$y(l_\xi) = y_0, \quad (\text{B4})$$

where  $l_\xi \equiv \ln(\xi/a_0)$ .

In analogy to a 2D plasma, the dynamic dielectric constant at temperature  $T$  can be written as

$$\epsilon(\omega, T) = \epsilon_b(\omega, T) + i\sigma_f(T)/\omega. \quad (\text{B5})$$

Via a Fokker-Planck equation approach, the vortex pair part is given by [25–27]

$$\epsilon_b(\omega, T) = 1 + \int_{a_0}^{\xi(T)} dr \frac{d\tilde{\epsilon}}{dr} \tilde{g}(r, \omega), \quad (\text{B6})$$

where  $a_0$  is the vortex core diameter. Here  $\tilde{g}(r, \omega)$  is a response function obeying the following second-order differential equation with respect to  $r$ :

$$r^2 \frac{d^2 \tilde{g}}{dr^2} + (3 - \eta) r \frac{d\tilde{g}}{dr} - \left( -i \frac{\omega}{\omega_0} \frac{r^2}{a_0^2} e^{-2l_D} + \eta \right) \tilde{g} + \eta = 0, \quad (\text{B7})$$

where  $l_D$  is defined in Eq. (20) and  $\eta(r) = 4T_c \tilde{\epsilon}(\infty, T_c) / [T \tilde{\epsilon}(r, T)]$ . In Refs. [25–27], the following approximate formula was used for  $\epsilon_b(\omega)$ :

$$\begin{aligned} \text{Re} \epsilon_b(\omega) &= \tilde{\epsilon}(\sqrt{14D/\omega}), \\ \text{Im} \epsilon_b(\omega) &= \frac{\pi}{4} \sqrt{\frac{14D}{\omega}} \tilde{\epsilon}'(\sqrt{14D/\omega}), \end{aligned}$$

where  $\tilde{\epsilon}'(r) \equiv d\tilde{\epsilon}(r)/dr$ . However, in our calculations, we will avoid such approximations and solve Eqs. (B6) and (B7)

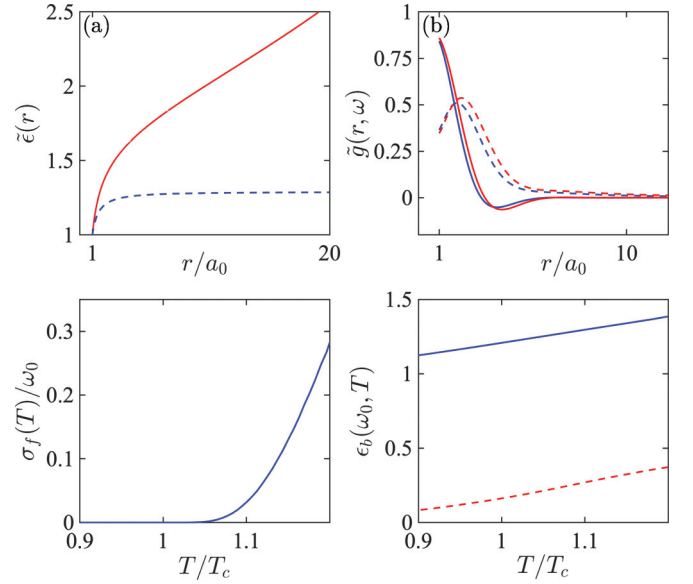


FIG. 5. (a)  $\tilde{\epsilon}(r)$  calculated for  $K_0 = 1$  (solid) corresponding to  $T < T_c$  and  $K_0 = 1.1$  (dashed) corresponding to  $T > T_c$ . (b) Real (solid) and imaginary (dashed) parts of  $\tilde{g}(r)$  calculated for  $K_0 = 1$  (blue) and  $K_0 = 1.1$  (red). (c)  $\xi(T)$  as a function of  $T/T_c$ . (d) Real (solid) and imaginary (dashed) parts of  $\epsilon_b(\omega_0, T)$  as a function of  $T/T_c$ . Here  $l_D = -0.5$ .

exactly. The free vortex contribution is found to be [25–27]

$$\sigma_f = \left( \frac{2\pi\hbar}{m} \right)^2 \left( \frac{D\rho_s^0}{k_B T} \right) n_f = 2\pi^2 \omega_0 K_0 e^{2l_D} \frac{a_0^2}{\xi^2}, \quad (\text{B8})$$

where  $n_f = 1/\xi^2(T)$  is the density of free vortices and  $K_0 = (\hbar/m)^2 \rho_s^0 / (k_B T)$  is the bare coupling constant. Naturally, no free vortex exists below  $T_c$ , i.e.,  $n_f = 0$  for  $T < T_c$ .

In Fig. 5 we show calculated examples of  $\tilde{\epsilon}(r)$ ,  $\tilde{g}(r)$ ,  $\sigma_f(T)$ , and  $\epsilon_b(\omega, T)$  for a weakly interacting 2D Bose gas with the dimensionless coupling constant  $g = 0.16$ . The obtained  $\epsilon_b(\omega, T)$  and  $\sigma_f$  are then used in the main text to determine the sound dispersion.

### APPENDIX C: THERMODYNAMIC QUANTITIES OF THE 2D WEAKLY INTERACTING BOSE GAS

For a weakly interacting 2D Bose gas, the various thermodynamic quantities, such as  $s$ ,  $\kappa_s$ ,  $\kappa_T$ , and  $c_v$ , can be calculated in terms of certain universal functions dependent only on the variable  $x = \mu/T$  and the dimensionless coupling constant  $g$ . First, all these quantities can be expressed in terms of the dimensionless reduced pressure  $\mathcal{P}$  and the phase space density  $\mathcal{D}$  [19]:

$$\mathcal{P}(x, g) \equiv \lambda_T^2 \frac{P}{T}, \quad \mathcal{D}(x, g) \equiv \lambda_T^2 \frac{\rho}{m}, \quad (\text{C1})$$

where  $\lambda_T = \hbar\sqrt{2\pi/mT}$  is the thermal de Broglie wavelength. More specifically, we have [19]

$$\begin{aligned} \bar{s} &= 2 \frac{\mathcal{P}}{\mathcal{D}} - x, & \bar{c}_v &= 2 \frac{\mathcal{P}}{\mathcal{D}} - \frac{\mathcal{D}}{\mathcal{D}'}, \\ \kappa_T &= \frac{m}{\rho T} \frac{\mathcal{D}'}{\mathcal{D}}, & \kappa_s &= \frac{m}{\rho T} \frac{\mathcal{D}}{2\mathcal{P}}, \end{aligned} \quad (\text{C2})$$

where  $\mathcal{D}' \equiv d\mathcal{D}/dx$ ,  $\bar{s} = ms$  is the entropy per particle and  $\bar{c}_v = mc_v$  specific heat capacity per particle. Since we are interested in the temperature dependence of many physical quantities, it is convenient to measure the temperature in terms of the BKT transition temperature  $T_c$ . For a gas with fixed density, it is easy to see from Eq. (C1) that

$$\frac{T}{T_c} = \frac{\mathcal{D}(x_c, g)}{\mathcal{D}(x, g)}, \quad (\text{C3})$$

where  $x_c = \frac{\pi}{g} \ln\left(\frac{\xi_\mu}{g}\right)$  with  $\xi_\mu = 13.2$  is the value of the  $x$  variable at the BKT transition point. Now, both  $\mathcal{P}$  and  $\mathcal{D}$  can be expressed in terms of a universal function  $\theta(x, g)$  as [37,38]

$$\mathcal{D}(x, g) = \pi \left[ \frac{x}{g} + \theta(x, g) \right] \quad (\text{C4})$$

and

$$\begin{aligned} \mathcal{P}(x, g) = & \mathcal{P}_c + \ln\left(\frac{\xi_\mu}{g}\right)(x - x_c) + \frac{\pi}{2g}(x - x_c)^2 \\ & + \frac{\pi g}{2}[\theta^2(x, g) - \theta^2(x_c, g)] - g[\theta(x, g) - \theta(x_c, g)], \end{aligned} \quad (\text{C5})$$

where  $\mathcal{P}_c$  is the reduced pressure at the critical point and can be calculated by the Hartree-Fock mean-field theory [39]. For the temperature range of our interest, the  $\theta$  function can be determined analytically by solving the equation [37,38]

$$\theta(x, g) - \frac{1}{\pi} \ln \theta(x, g) = \frac{1}{g}(x - x_c) + \frac{1}{\pi} \ln(2\xi_\mu). \quad (\text{C6})$$

The static superfluid density  $\rho_s(0)$  can be expressed in terms of another dimensionless quantity:

$$\mathcal{D}_s(x, g) = \lambda_T^2 \frac{\rho_s(0)}{m}. \quad (\text{C7})$$

This latter is given by

$$\mathcal{D}_s = 2\pi\theta - 1 \quad (\text{C8})$$

for  $\frac{x-x_c}{g} > 0.5$  and

$$\frac{4}{\mathcal{D}_s} + \ln \frac{\mathcal{D}_s}{4} = 1 + 0.61 \frac{x - x_c}{g} \quad (\text{C9})$$

for  $-0.1 < \frac{x-x_c}{g} < 0.5$ .

- 
- [1] N. D. Mermin, *Rev. Mod. Phys.* **51**, 591 (1979).  
[2] V. Berezinsky, *Sov. Phys. JETP* **32**, 493 (1971).  
[3] J. M. Kosterlitz and D. J. Thouless, *J. Phys. C* **5**, L124 (1972).  
[4] J. M. Kosterlitz and D. J. Thouless, *J. Phys. C* **6**, 1181 (1973).  
[5] J. V. José, L. P. Kadanoff, S. Kirkpatrick, and D. R. Nelson, *Phys. Rev. B* **16**, 1217 (1977).  
[6] J. M. Kosterlitz, *Rep. Prog. Phys.* **79**, 026001 (2016).  
[7] D. J. Bishop and J. D. Reppy, *Phys. Rev. Lett.* **40**, 1727 (1978).  
[8] D. J. Bishop and J. D. Reppy, *Phys. Rev. B* **22**, 5171 (1980).  
[9] A. F. Hebard and A. T. Fiory, *Phys. Rev. Lett.* **44**, 291 (1980).  
[10] Z. Hadzibabic, P. Krüger, M. Cheneau, B. Battelier, and J. Dalibard, *Nature (London)* **441**, 1118 (2006).  
[11] P. A. Murthy, I. Boettcher, L. Bayha, M. Holzmann, D. Kedar, M. Neidig, M. G. Ries, A. N. Wenz, G. Zürn, and S. Jochim, *Phys. Rev. Lett.* **115**, 010401 (2015).  
[12] Z. Hadzibabic and J. Dalibard, *Rivista del Nuovo Cimento*, **34**, 389 (2011).  
[13] T. Mishonov and A. Groshev, *Phys. Rev. Lett.* **64**, 2199 (1990).  
[14] O. Buisson, P. Xavier, and J. Richard, *Phys. Rev. Lett.* **73**, 3153 (1994).  
[15] K. R. Atkins, *Phys. Rev.* **113**, 962 (1959).  
[16] D. Bergman, *Phys. Rev.* **188**, 370 (1969).  
[17] R. S. Kagiwada, J. C. Fraser, I. Rudnick, and D. Bergman, *Phys. Rev. Lett.* **22**, 338 (1969).  
[18] J. L. Ville, R. Saint-Jalm, E. Le Cerf, M. Aidelsburger, S. Nascimbène, J. Dalibard, and J. Beugnon, *Phys. Rev. Lett.* **121**, 145301 (2018).  
[19] T. Ozawa and S. Stringari, *Phys. Rev. Lett.* **112**, 025302 (2014).  
[20] X.-J. Liu and H. Hu, *Ann. Phys.* **351**, 531 (2014).  
[21] M. Ota and S. Stringari, *Phys. Rev. A* **97**, 033604 (2018).  
[22] M. Ota, F. Larcher, F. Dalfovo, L. Pitaevskii, N. P. Proukakis, and S. Stringari, *Phys. Rev. Lett.* **121**, 145302 (2018).  
[23] A. Cappellaro, F. Toigo, and L. Salasnich, *Phys. Rev. A* **98**, 043605 (2018).  
[24] V. P. Singh and L. Mathey, *Phys. Rev. Research* **2**, 023336 (2020).  
[25] V. Ambegaokar, B. I. Halperin, D. R. Nelson, and E. D. Siggia, *Phys. Rev. Lett.* **40**, 783 (1978).  
[26] V. Ambegaokar and S. Teitel, *Phys. Rev. B* **19**, 1667 (1979).  
[27] V. Ambegaokar, B. I. Halperin, D. R. Nelson, and E. D. Siggia, *Phys. Rev. B* **21**, 1806 (1980).  
[28] P. Minnhagen, *Rev. Mod. Phys.* **59**, 1001 (1987).  
[29] L. Pitaevskii and S. Stringari, *Bose-Einstein Condensation* (Oxford University Press, New York, 2003).  
[30] A. Griffin and E. Zaremba, *Phys. Rev. A* **56**, 4839 (1997).  
[31] M. R. Andrews, D. M. Kurn, H.-J. Miesner, D. S. Durfee, C. G. Townsend, S. Inouye, and W. Ketterle, *Phys. Rev. Lett.* **79**, 553 (1997).  
[32] D. M. Stamper-Kurn, H.-J. Miesner, S. Inouye, M. R. Andrews, and W. Ketterle, *Phys. Rev. Lett.* **81**, 500 (1998).  
[33] R. Meppelink, S. B. Koller, and P. van der Straten, *Phys. Rev. A* **80**, 043605 (2009).  
[34] E. Taylor, H. Hu, X.-J. Liu, L. P. Pitaevskii, A. Griffin, and S. Stringari, *Phys. Rev. A* **80**, 053601 (2009).  
[35] J. Joseph, B. Clancy, L. Luo, J. Kinast, A. Turlapov, and J. E. Thomas, *Phys. Rev. Lett.* **98**, 170401 (2007).  
[36] L. A. Sidorenkov, M. K. Tey, R. Grimm, Y.-H. Hou, L. Pitaevskii, and S. Stringari, *Nature (London)* **498**, 78 (2013).  
[37] N. Prokof'ev, O. Ruebenacker, and B. Svistunov, *Phys. Rev. Lett.* **87**, 270402 (2001).  
[38] N. Prokof'ev and B. Svistunov, *Phys. Rev. A* **66**, 043608 (2002).  
[39] T. Yefsah, R. Desbuquois, L. Chomaz, K. J. Günter, and J. Dalibard, *Phys. Rev. Lett.* **107**, 130401 (2011).  
[40] P. Minnhagen and M. Nylén, *Phys. Rev. B* **31**, 5768 (1985).